Three-Dimensional Drift Kinetic Response of High-β Plasmas in the DIII-D Tokamak

Z. R. Wang, M. J. Lanctot, Y. Q. Liu, J-K. Park, and J. E. Menard

Phys. Rev. Lett. **114**, 145005 — Published 7 April 2015

DOI: 10.1103/PhysRevLett.114.145005

Three-dimensional drift kinetic response of high beta plasmas in the DIII-D tokamak

Z.R. Wang,[1] M.J. Lanctot,[2] Y.Q. Liu,[3] J-K. Park,[1] and J.E. Menard[1]

[1]*Princeton Plasma Physics Laboratory Princeton, New Jersey 08543, USA*
[2]*General Atomics, PO Box 85608, San Diego, CA 92186-5608, USA*
[3]*Culham Centre for Fusion Energy, Culham Science Centre, Abingdon, OX14 3DB, United Kingdom*

(Dated: February 4, 2015)

A quantitative interpretation of the experimentally measured high pressure plasma response to externally applied three-dimensional (3D) magnetic field perturbations, across the no-wall Troyon β limit, is achieved. The self-consistent inclusion of the drift kinetic effects in magneto-hydrodynamic (MHD) modeling[1] succesfully resolves an outstanding issue of ideal MHD model, which significantly over-predicts the plasma induced field amplification near the no-wall limit, as compared to experiments. The model leads to quantitative agreement not only for the measured field amplitude and toroidal phase, but also for the measured internal 3D displacement of the plasma. The results can be important to the prediction of the reliable plasma behavior in advanced fusion devices, such as ITER [2].

PACS numbers: 52.25.Dg 52.55.Fa 52.65.Ww

Externally applied, non-axisymmetric magnetic perturbations can strongly modify tokamak plasmas, leading to a three-dimensional (3D) equilibrium. The 3D field consists of the applied field and the perturbation due to the perturbed plasma currents [3–5], termed the plasma response. The plasma response has been systematically observed for about a decade in tokamak devices e.g. DIII-D[6–10], JET[11], NSTX [12, 13] and other fusion experimental devices such as reversed field pinch [14], and large helical device[15]. In tokamaks, the plasma response may significantly amplify the applied field, resulting in the neoclassical toroidal viscosity (NTV) [16–18] and degradation of plasma performance such as the energetic particle losses[19] and MHD instabilities [20, 21] in present tokamaks and ITER [2]. Since the initial analytic work by Boozer [5], various attempts have been made for quantitative modelling of this phenomenon at high pressure[6, 22], with limited success.

In this letter, the drift kinetic effects, derived from the perturbed drift kinetic theory and associated with distorted particle orbits by 3D fields [23–25], have, for the first time, explained the observed beta dependence of plasma response in the vicinity of the ideal MHD predicted no-wall β limit, denoted as β^{NW} [26], where $\beta = 2\mu_0\langle p\rangle/B_0^2$, $\langle p\rangle$ is the volume-averaged plasma pressure, B_0 is the magnetic strength at plasma center, and μ_0 is the magnetic permeability. A long standing issue in plasma response physics is that ideal MHD theory finds a nearly singular amplification of response near β^{NW} due to the ideal potential energy approaching zero when β approaches β^{NW}. In contrast, empirical experiments show the linear increase of plasma response across β^{NW}. This disagreement is studied through a quantitative comparison between DIII-D experimental results [10] and the accurate modeling results obtained by solving the linear hybrid drift-kinetic MHD equation[1]. Since the kinetic effects can dramatically modify the plasma response

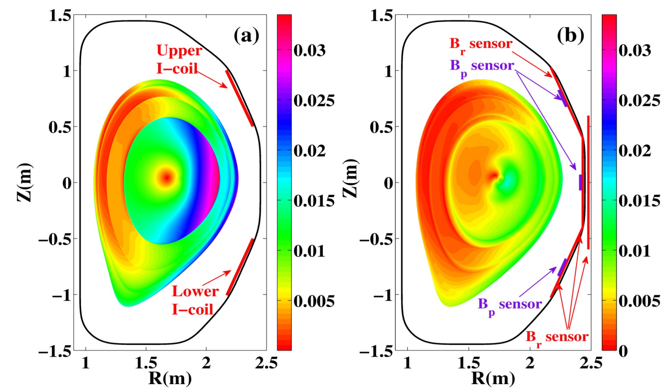

FIG. 1. Comparison of the computed amplitude (cm/kA) of the radial plasma displacement from DIII-D discharge 135773, assuming (a) the fluid model, and (b) the kinetic model. The geometry of magnetic sensors, upper and lower I-coils, and the modelled resistive wall are also shown.

structure, the results also highlight the importance of solving the model equations self-consistently. Only in a self-consistent calculation, the kinetic effects can modify the response structure (i.e. displacement).

To study the plasma response in DIII-D experiments, an external n=1 traveling perturbation with 10Hz rotating frequency is applied by the upper and lower Internal coil (I-coil) arrays with a toroidal phase difference $\Delta\phi = 240$ degrees [10]. Neutral beam injection (NBI) in the plasma current direction is used to control normalized beta, $\beta_N = \beta(\%)/[I_p(\mathrm{MA})/a(\mathrm{m})B_0(\mathrm{T})]$, where I_p is the plasma current and a is the plasma minor radius. β_N^{NW} is the normalized β^{NW}. To investigate the β dependence of plasma response, the β_N value of the concerned discharges (135762, 135761, 135758, 135765, 135773, 135759) at 1800ms is varied from 1.14 to 2.40. The experimental details are presented in [10, 27]. The magnetic perturbation due to plasma response is defined as $\delta\vec{B}^{plas}$(Gauss/kA)= $(\delta\vec{B}^{tot}(\text{Gauss})-\delta\vec{B}^{ext}(\text{Gauss}))/I_c(\text{kA})$, and is measured by the magnetic sensor on the low field side. Here, $\delta\vec{B}^{tot}$ is the total perturbed field. $\delta\vec{B}^{ext}$ is the non-axisymmetric magnetic perturbation applied by I-coils with the coil current I_c. Figure 1 illustrate the geometry of I-coils and magnetic sensors.

Since $\delta\vec{B}^{tot}$ is small compared to the equilibrium magnetic field $\vec{B}$ in the experiments, $\delta B^{tot}/B < 10^{-3}$, the comparative results against experiments in this work demonstrate that the linear perturbation theory is largely valid for studying 3D plasma response. The linear response eventually results from the linear combination of plasma eigenmode solutions. For instance, the response typically results from a single, damped, long-wavelength kink mode driven by the perturbation. Two versions of the MARS code are employed in this work. The MARS-K code solves the linearized ideal single-fluid MHD equations with drift kinetic effects in the so called non-perturbative approach [1, 28], where the vacuum, the external coils and the modelled resistive wall (vacuum vessel) as shown in Fig. 1 are included into the computations [4]. MARS-K is capable of modeling the plasma response experiment by computing the response with self-consistent inclusion of the kinetic effects, yielding the so-called kinetic plasma response. MARS-F only solves the linearized ideal MHD equations to obtain the fluid plasma response [10]. The upgraded MARS-K/F codes, with improved numerical stability, have been benchmarked with IPEC-PENT code [29, 30] and MISK code [31].

Figure 1 compares the computed radial plasma displacement $\vec{\xi}\cdot\nabla s$ between the fluid and the kinetic approaches, based on DIII-D discharge 135773, where the plasma pressure is close to the $\beta_N^{NW} = 2.25$. Here $s \equiv \sqrt{\psi}$ with ψ being the normalized equilibrium poloidal flux [32, 33]. In computing the kinetic plasma response, the equilibrium distribution function of thermal particles (TPs, both ions and electrons) is assumed to be Maxwellian. The energetic particles (EPs), due to NBI, are modeled with an isotropic slowing down distribution, with the fast ion pressure and density computed by the TRANSP code. Both TPs and EPs contribute adiabatic and non-adiabatic perturbed pressures [1]. In particular, the non-adiabatic contributions come from the resonant kinetic effects associated with the particle's toroidal precession, bounce (for trapped particles) and transit (for passing particles) motions [1]. The TPs are assumed to be collisional with the Crook operator as defined in [25], whereas the EPs are collisionless. In Fig. 1(b), the plasma response includes all the aforementioned kinetic contributions. Compared with the fluid response shown in Fig. 1(a), the response amplitude is strongly suppressed by the kinetic effects which significantly modify the internal structure of the response near the plasma core at the low field side (LFS).

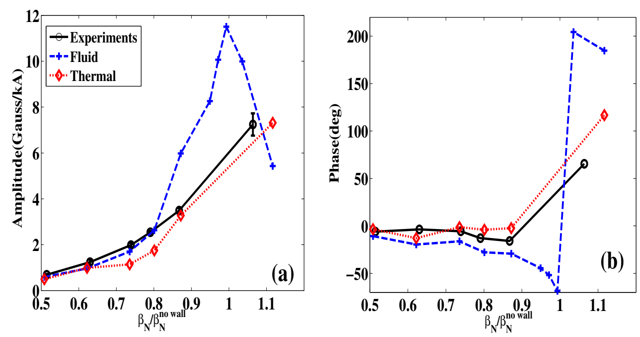

FIG. 2. The *beta* dependence of (a) amplitude and (b) toroidal phase of the response field (δB_r^{plas}) through the magnetic sensors. The computed response, with the fluid model (dashed), and with the kinetic model including thermal particles (diamond), is compared with the experimental data ('o').

The measured amplitude and toroidal phase of δB_r^{plas}, by the radial magnetic sensors located at the LFS midplane, are compared in Fig.2 with that computed by MARS-F/K. As a subtle point, the wall time of the DIII-D vacuum vessel has been calibrated in MARS-F/K, by comparing the computed wall response to the applied ac fields with frequency scan, with that measured in the vacuum experiments. In Fig.2, the fluid response agrees well with experiments for $\beta_N/\beta_N^{NW} < 0.81$, suggesting that the fluid approximation is adequate for modeling the plasma response at low beta [10]. This is also supported by the modeling results for MAST plasmas [34]. However, the disagreement between the ideal MHD prediction and experiments appears as the pressure approaches or exceeds β_N^{NW}. Especially, at $\beta_N > \beta_N^{NW}$, ideal MHD predicts an unstable $n = 1$ resistive wall mode (RWM), while the experiments remain stable. For computing the fluid response near β_N^{NW} (β_N/β_N^{NW} from 0.94 to 1.04), we scale the pressure based on the equilibria from discharges 135773 and 135759 with $\beta_N/\beta_N^{NW} = 0.87$ and 1.06 respectively. The nearly singular amplification of the fluid response close to the no-wall limit is due to the fact that the perturbed potential energy $\delta W = \delta W_p + \delta W_{vac}$ approaches zero at β_N^{NW} [12], where δW_p is the plasma potential energy, δW_{vac} is the vacuum energy, the stable plasma has $\delta W>0$. When $\beta_N > \beta_N^{NW}$, the steady state fluid response losses physics meaning due to RWM instability, although MARS-F can still compute such a response (by direct inversion of the system matrix). The amplitude of the fluid response quickly decreases since δW becomes finite again. Equally interesting observation is a significant toroidal phase change (greater than 180 degrees) of the response since δW switches sign. In contrast, the experimental plasma remains stable. The measured amplitude of the plasma response almost linearly increases with β_N across β_N^{NW}, with 65 degrees less toroidal phase than the fluid response. The disagree-

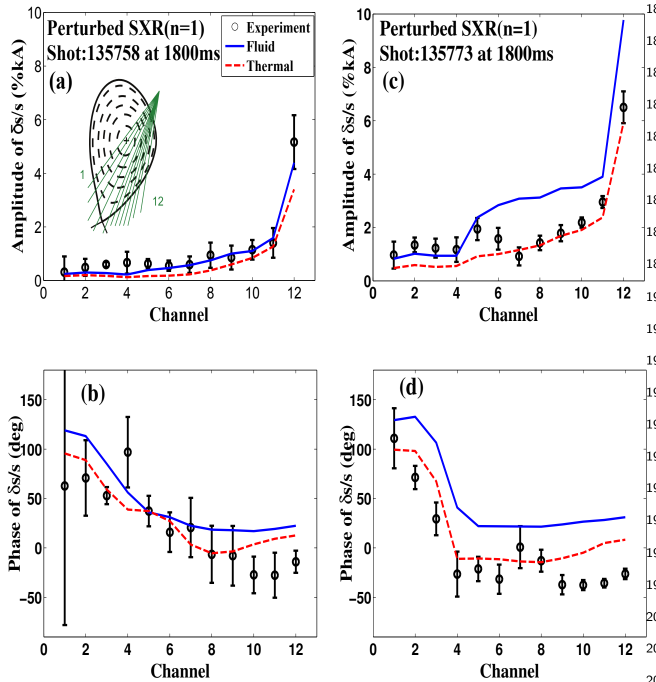

FIG. 3. Comparison of SXR amplitude (a),(c) and phase (b),(d) between the measured ('o') and computed n=1 response, where the computed 'fluid' (solid) and 'thermal' (dashed) cases are considered. Two cases are shown: (a),(b) with $\beta_N/\beta_N^{NW} = 0.74$ (135758) and (c),(d) with $\beta_N/\beta_N^{NW} = 0.87$ (135773). The inset in (a) shows the SXR sightline geometry of each channel.

ment between the ideal MHD prediction and experiments points to the need for additional physics, such as the kinetic effects [5, 12, 27], in determining the plasma response.

Much better agreement is obtained by the kinetic response computations. The first example (termed 'thermal') is reported in Fig. 2, where the adiabatic contributions from both TPs and EPs are included, but the non-adiabatic term includes the TPs contribution only. The dominant role of TPs on the kinetic response is examined later on. The kinetic response computations were only performed for equilibria reconstructed from experiments, i.e. no pressure scaling near β_N^{NW} as has been made for the fluid response computations. This is because the drift kinetic computations require additional experimental profiles that cannot be simply scaled, such as the $E \times B$ rotation, the pressure profile of EPs, etc. The kinetic response significantly improves agreement with experiments near or above β_N^{NW} due to several factors. (i) The kinetic effects modify the plasma response structure as shown in Fig. 1, which also changes δW. (ii) The kinetic effects result in a complex dissipative kinetic energy δW_K [35] which acts to maintain a finite response amplitude as the pressure approaches or exceeds the no-wall limit. (iii) The finite imaginary part of δW_K also reduces the toroidal phase shift compared to that of the fluid response, leading to a much closer agreement (of the kinetic response) to experiments. (iv) Finally, the hybrid kinetic-MHD theory predicts stable RWM in the highest β case (135759), which is consistent with the experimental observation. Similarly, the kinetic response also shows the reliable agreement with NSTX plasma response experiments which cannot be predicted by the fluid response [36].

We also note that the present kinetic computations tend to slightly underestimate the experimental response amplitude at low beta $0.7 < \beta_N/\beta_N^{NW} < 0.9$. This may point to certain missing physics in our present kinetic model. One likely candidate is the perturbed electrostatic potential which is neglected in MARS-K. The uncertainties in the reconstructed plasma edge rotation may also contribute to this discrepancy.

Another crucial validation of the kinetic response model is the direct comparison of the computed and measured internal response structure. In experiments, the internal structure is derived from the soft x-ray (SXR) measurement [37]. This is compared with computations in Fig. 3 for two discharges. The experimental data are represented by a quantity $\delta s/s$, measured at 12 SXR channels shown in Fig. 3(a), where the equilibrium (n=0) SXR measurement, s(m), and the n=1 component of the SXR perturbation, δs(m/kA), are both integral quantities along the sightline of each channel. This quantity is compared to the internal structure of the n=1 plasma response predicted by MARS-F/K via modeling of the SXR measurements. Details of modeling are described in [27]. In Fig. 3, the experimental data are time-averaged over 400ms (4 cycles of SXR) around 1800ms. The error bars are obtained from an error analysis of the data fitting. The simulated SXR signals, for the 'fluid' and 'thermal' cases, are based on the computed normal displacement of the plasma response. The phase of $\delta s/s$ is defined with reference to $\delta\vec{B}^{ext}$ of upper I-coils. For the low β case ($\beta_N/\beta_N^{NW} = 0.74$), both fluid and kinetic computations show agreement with experiments, for both amplitude and phase of the n=1 internal structure. We note that the largest perturbed amplitude appears near the plasma edge (channel 12). For the case near the no-wall limit ($\beta_N/\beta_N^{NW} = 0.87$), the fluid response largely overestimates the amplitude of the internal perturbation along channels 6 to 12. The phase of the fluid response also disagrees with measurements. The kinetic response ('thermal' case), on the other hand, generally shows very good quantitative agreement with DIII-D experiments, for both amplitude and phase. The above comparison again indicates that the kinetic effects play an important role in the high beta plasma response. The self-consistent hybrid drift-kinetic MHD theory is further validated by this sophisticated SXR comparison. It is noted that this modification of plasma response by kinetic effects near β_N^{NW} can be critical to many important applications such

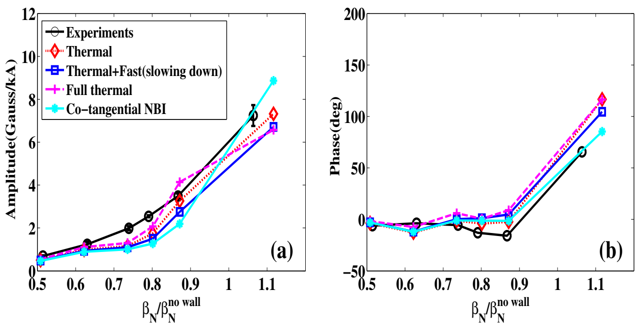

FIG. 4. The β dependence of (a) amplitude and (b) toroidal phase of δB_r^{plas}. The experimentally measured δB_r^{plas} is compared with the computed kinetic response of 'thermal' (diamond), 'thermal+fast' (square), 'full thermal' ('+') and 'co-tangential NBI' ('$*$') cases

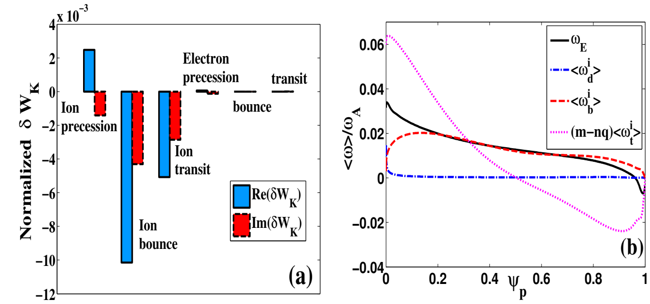

FIG. 5. (a) The real and imaginary parts of normalized δW_K contributed by different resonances of thermal ions and electrons. (b) The radial profiles of ω_E (solid) and various averaged frequencies of trapped and passing thermal ions over the velocity space and the flux surface, such as $\langle\omega_d^i\rangle$ (dash-dot), $\langle\omega_b^i\rangle$ (dashed) and $(m-nq)\langle\omega_t^i\rangle$ (dotted) of thermal ions. All frequencies are normalized by the Alfvén frequency ω_A at the plasma center.

as NTV torque, which has the quadratic dependence on the perturbed field and the displacement. For instance, figure 3 (c) implies the fluid response might predict four time larger NTV torque than the more accurate kinetic response.

Further MARS-K computations reveal that the kinetic effects from thermal particles play the major role in reproducing the experimental plasma response. Figure 4 compares results under various assumptions on the particle contributions. By adding the non-adiabatic contributions from EPs on top of "thermal" case, termed "thermal+fast", we find negligible impact of EPs on the kinetic response. On the other hand, by assuming that all the equilibrium pressure comes from TPs (termed "full thermal" case), the kinetic response shows similar behavior as that of the "thermal" case. Near the no-wall limit, the response amplitude in the "full thermal" case is slightly larger than that of the other two cases, due to the lack of one extra adiabatic term arising from the boundary integration in the particle phase space for the slowing down EPs with finite birth energy [28]. This extra term eventually plays a damping role. Further comparison of the SXR based internal structure again confirms the importance of thermal particle contribution, at least for these DIII-D plasmas. In experiments, co-tangential NBI was employed, with two injection tangency radii of 76cm and 115cm, producing EPs with anisotropic distributions in the particle pitch angle space. This motivates us to test the sensitivity of kinetic response against the EP models. MARS-K has implemented an anisotropic NBI model which is suitable for ITER [28]. We choose an averaged injection tangency radii of 95.5cm and an ITER-like beam width parameter ($\delta\zeta = 0.123$). The results, termed "co-tangential NBI" in Fig. 4, show that the plasma response has a larger amplitude than other cases due to the destabilizing effect of EPs and a better phase agreement with experiments at $\beta_N/\beta_N^{NW} = 1.12$. It implies experimentally more relevant NBI models should be implemented in the future to better capture the EPs kinetic effects at high beta. Nevertheless, for these DIII-D plasmas, the TPs contribution is still dominant, and the modeled monotonic increase of the response amplitude with pressure is qualitatively unchanged by the anisotropic EP model.

A deeper understanding of the kinetic response physics is gained by the energy analysis shown in Fig. 5(a), where we compare the non-adiabatic kinetic contributions from both thermal ions and electrons, in various resonance regimes including toroidal precession and bounce resonance of trapped particles, as well as transit resonance of passing particles. We choose discharge 135773 with $\beta_N/\beta_N^{NW} = 0.87$ to illustrate these physics. Figure 5(a) presents the real and imaginary parts of δW_K associated with the aforementioned kinetic contributions. These energy components are normalized by the plasma volume integrated inertia $\delta K = \int \rho(\xi \cdot \nabla s)^2 dV$, where ρ is the mass density. The comparison shows that thermal electrons contribute much less δW_K than thermal ions, since the former have much higher collision, bounce, and transit frequencies than the latter. Moreover, we find that the precession, bounce and transit resonances of thermal ions contribute comparable amounts of δW_K, indicating that three types of resonances from TPs are important for the kinetic response. The eventual response depends on the net contribution, after possible cancellations among all energy components. In Fig. 5(b), the frequency comparison confirms the energy analysis results. It is clear that the $E \times B$ rotation can always be in local resonance with all types of particle drift motions, due to the energy dependence of particle drift frequencies [38]. Indeed, ω_E can match, at different flux surfaces, the averaged precession frequency $\langle\omega_d^i\rangle$, the bounce frequency $\langle\omega_b^i\rangle$, as well as the transit frequency $(m-nq)\langle\omega_t^i\rangle$ of thermal ions, where m is the poloidal mode number, q is the safety factor. The harmonic numbers $l = 1$, $m = 2$ and $n = 1$ are chosen because these belong to the dominant harmonics contributing to the plasma response.

In summary, kinetic response resolves the long-standing disagreement between the fluid theory prediction and the experimental observations, as long as the plasma pressure approaches or exceeds the no-wall limit. Quantitative comparison between the measured $n = 1$ plasma response (both external and internal data), and the computational results, reveals the key importance of kinetic effects from TPs. Kinetic response leads to internal structure that is different from the fluid response throughout the plasma. The energy analysis shows that the modification of the response is mainly contributed by the precession, bounce and transit resonances of thermal ions in these DIII-D plasmas. These results demonstrate the validity of the hybrid drift-kinetic MHD model, and highlight the necessity of self-consistent approach as the only viable way for achieving quantitative modeling of 3D plasma response in high beta tokamak plasmas.

This material is based upon work supported by the U.S. Department of Energy, Office of Science, Office of Fusion Energy Sciences, using the DIII-D National Fusion Facility, a DOE Office of Science user facility, under Award DE-FC02-04ER54698, and DE-AC02-09CH11466. DIII-D data shown in this paper can be obtained in digital format by following the links at `https://fusion.gat.com/global/D3D_DMP`. This project has also received funding from the European Union's Horizon 2020 research and innovation programme under grant agreement number 633053 and from the RCUK Energy Programme [grant number EP/I501045]. The views and opinions expressed herein do not necessarily reflect those of the European Commission. M.J. Lanctot and Z.R. Wang thank Dr. Jeremy Hanson for his help in analyzing the vacuum coil-sensor transfer functions. We thank Dr. Ted Strait for valuable comments on the manuscript. M.J. Lanctot also acknowledges Columbia University for support while obtaining the plasma response measurements described herein.

[1] Y.Q. Liu et al., Phys. Plasmas **15**, 112503 (2008).
[2] K. Ikeda., Nucl. Fusion. **47**, S1 (2007).
[3] J.-K Park, A.H. Boozer and A.H. Glasser, Phys. Plasmas **14**, 052110 (2007).
[4] Y.Q. Liu, A. Kirk and E. Nardon, Phys. Plasmas **17**, 122502 (2010).
[5] A.H. Boozer, Phys. Rev. Lett. **86**, 22 (2001).
[6] A.M. Garofalo, T.H. Jensen and E.J. Strait , Phys. Plasmas **10**, 056112 (2003).
[7] A.M. Garofalo et al., Phys. Rev. Lett. **82**, 3811 (1999).
[8] H. Reimerdes et al., Phys. Rev. Lett. **93**, 135002 (2004).
[9] H. Reimerdes et al., Phys. Plasmas **13**, 056107 (2006).
[10] M.L. Lanctot et al., Phys. Plasmas **17**, 030701 (2010).
[11] T. Hender et al 2006 Prediction of rotational stabilisation of resistive wall modes in ITER Proc. 21st IAEA Fusion Energy Conf. 2006 (Chengdu, China, 2006) (Vienna: IAEA) IAEA-CN-149/ EX/P8-18 CD-ROM file EX/P8-18
[12] J.-K. Park et al., Phys. Plasmas **16**, 082512 (2009).
[13] S.A. Sabbagh et al., Nucl. Fusion **53**, 104007 (2013).
[14] P. Piovesan et al., Plasma Phys. Control. Fusion **53** 084005 (2011).
[15] K. Narlhara et al. Phys. Rev. Lett. **87** 135002 (2001).
[16] J.-K. Park, Phys. Rev. Lett. **111**, 095002 (2013).
[17] J.D. Callen, Nucl. Fusion **51**, 094026 (2011).
[18] K.C. Shaing., Phys. Fluids **26**, 3315 (1983).
[19] M. Garcia-Munoz et al., Plasma Phys. Control. Fusion **55**, 124014 (2013).
[20] R.J. Buttery et al., Nucl. Fusion **51**, 073016 (2011).
[21] H. Reimerdes et al., Nucl. Fusion **49**, 115001 (2009).
[22] J.W. Berkery et al., Phys. Plasmas **21**, 056112 (2014).
[23] T. M. Antonsen and Y. C. Lee, Phys. Fluids **25**, 132 (1982).
[24] F. Porcelli et al., Phys. Plasmas **1**, 470 (1994).
[25] J.-K. Park et al., Phys. Rev. Lett. **102**, 065002 (2009).
[26] F. Troyon et al., Plasma Phys. Control. Fusion **26**, 209 (1984).
[27] M.L. Lanctot et al., Phys. Plasmas **18**, 056121 (2011).
[28] Y.Q. Liu et al., Phys. Plasmas **21**, 056105 (2014).
[29] Z.R. Wang et al., Phys. Plasmas **21**, 042502 (2014).
[30] N.C. Logan et al., Phys. Plasmas **20**, 122507 (2013).
[31] J.W. Berkery et al., Phys. Plasmas **21**, 052505 (2014).
[32] D. Yadykin et al, Plasma Phys. Control. Fusion **53** 085024 (2011).
[33] Y.Q. Liu et al, Phys. Plasmas **17**, 122502(2010).
[34] Y.Q. Liu et al., Nucl. Fusion **51**, 083002 (2011).
[35] B. Hu and R. Betti, Phys. Rev. Lett. **93**, 105002 (2004).
[36] Z.R. Wang et al, The role of drift kinetic effects and fluid flow on the plasma response in high-beta tokamak experiments, 19th MHD workshop 2014(Auburn University, USA).
[37] I. N. Bogatu et al., Rev. Sci. Instrum. **75**, 2832 (2004).
[38] Z.R. Wang, S.C. Guo and Y.Q. Liu, Phys. Plasmas **19**, 072518 (2012).
[39] J.-K. Park, Phys. Plasmas **18**, 110702(2011).